arXiv:astro-ph/9905206v1 17 May 1999

Outburst in the Polarized Structure of the Compact Jet of 3C 454.3

José-Luis Gómez

Instituto de Astrofísica de Andalucía, CSIC, Apartado 3004, 18080 Granada, Spain

Alan P. Marscher

Department of Astronomy, Boston University, 725 Commonwealth Avenue, Boston, MA 02215, USA

and

Antonio Alberdi

Instituto de Astrofísica de Andalucía, CSIC, Apartado 3004, 18080 Granada, Spain

Received _____; accepted _____

ABSTRACT

We present three-epoch polarimetric images of the quasar 3C 454.3 obtained with the Very Long Baseline Array at 22 and 43 GHz. 22 GHz polarized intensity images show a sudden change in the polarization structure of a bright eastern component (which we call the "core," although it may be neither at the upstream end of the jet nor completely stationary) over a 41-day interval, coincident with the ejection of a new component from the core, as resolved in the corresponding 43 GHz images. This polarization outburst is also present at 43 GHz in both the core and the new component. This may represent a rapid change in the electric vector position angle of the ejected component from being orthogonal to almost parallel to that of the core. About seven months later, the new component, moving superluminally at 2.9±0.4 $h^{-1}\,c$ ($q_\circ$=0.5) relative to the core and 3.9±0.4 $h^{-1}\,c$ relative to a bright stationary component about 0.6 mas west of the core — very low compared with previous measurements — is found at 43 GHz to exhibit a further rotation of 90° in the orientation of its polarization. Opacity effects may account for the first rotation, but changes in the magnetic field of the component and/or that of the underlying jet in the inner milliarcsecond structure of 3C 454.3 are needed to account for the second.

Polarized intensity images of the quasar 0420−014, used as a calibrator, are also presented. The polarization position angle of the core rotated between late 1994 and late 1996.

Subject headings: Polarization - Techniques: interferometric - galaxies: active - quasars: individual: 3C 454.3 - Galaxies: jets - Radio continuum: galaxies

1. Introduction

The quasar 3C 454.3 at redshift z=0.859 is one of the brightest extragalactic radio sources. It is an optically violent variable with a relatively high total linear polarization. It was the subject of the first polarimetric VLBI observation (Cotton et al. 1984) at a wavelength of 13 cm. Pauliny-Toth et al. (1987) presented the results of an extensive monitoring program of this source, covering about 5 yr of observations at 2.8 cm. These observations revealed the existence of superluminal components, with apparent proper motions between 0.21 and 0.35 mas yr^{-1}, or equivalently between 4.4 and 7.3 $h^{-1}c$ ($H_\circ$= 100 h km s^{-1} Mpc $^{-1}$, $q_\circ$=0.5), and a pair of quasi-stationary components, one situated at about 0.6 mas of the core, and a second one at about 1 mas, the latter of which was only detected from 1983.8 to 1984.9. A higher resolution polarimetric 6 cm VLBI map was presented by Cawthorne & Gabuzda (1996). This showed a curving jet with a magnetic field aligned with the jet axis, except for the inner component *K7* (which can be identified with the stationary component at 0.6 mas observed by Pauliny-Toth et al. 1987), whose magnetic field lay almost perpendicular to the direction of the jet flow. Kemball et al. (1996) presented the first polarimetric 7 mm Very Long Baseline Array (VLBA)[1] image of 3C 454.3. This revealed a three-component structure in polarized intensity, consisting of the core, the stationary component previously found by Pauliny-Toth et al. (1987) at 0.6 mas, and a new component located between both of these. This component was determined to have a polarization position angle almost perpendicular to the stationary component, which has a magnetic field perpendicular to the jet axis, as previously observed by Cawthorne & Gabuzda (1996). Marscher (1998) presented a sequence of eleven 43 GHz VLBA images covering two years of observations starting in

[1]The VLBA is an instrument of the National Radio Astronomy Observatory, which is a facility of the National Science Foundation operated under cooperative agreement by Associated Universities, Inc.

late 1994. A proper motion of 0.28 ± 0.02 mas yr^{-1} was observed for a component in the inner milliarsecond structure. These observations revealed no stationary component at the eastern end of the jet, but rather a weak, roughly stationary component 0.2 mas downstream of it. Further 5 and 8.4 GHz VLBI observations of 3C 454.3 were presented by Pauliny-Toth (1998), showing mean proper motions of 0.68 ± 0.02 mas yr^{-1} along a curved path at a distance of 2–4 mas from the "core."

2. Observations

We present three-epoch polarimetric observations of 3C 454.3 obtained with the VLBA. The first two observations were performed on 1996 November 11 and December 22 at 1.3 cm and 7 mm, in which 3C 454.3 served as a calibrator for 3C 120 (Gómez et al. 1998). The data were recordered in 1-bit sampling VLBA format with 32 MHz bandwidth per circular polarization. The reduction of the data was performed within the NRAO Astronomical Image Processing System (AIPS) software. The instrumental polarization was determined using the feed solution algorithm developed by Leppänen et al. (1995) on the source 0420-014. Comparison with other polarimetric observations carried out at similar epochs and frequencies revealed a good agreement in the determination of the D-terms (M. Lister, private communication), and were used to calibrate the electric-vector position angle (EVPA) with an error that we estimate to be within 10°. We also refer the readers to Gómez et al. (1998) for further details about the reduction and calibration of the data.

Figure 1 shows the VLBA images obtained for 0420-014. Only slight structural changes are observed between both frequencies and epochs. The total and polarized intensity images are dominated by a strong core component, with an EVPA in the east-west direction, which smoothly rotates toward the southwest, in the direction of the jet structure. This represents a rotation of the EVPA by about 45° with respect to that measured by Kemball et al. (1996)

two years previously, accompanied by a decrease in the peak percentage linear polarization to less than 2.2%.

The third 43 GHz polarimetric VLBA observation took place on 1997 July 30–31 as part of a γ-ray blazar monitoring program. The data analysis was similar to the previous two epochs, except that a component of 3C 279, with its EVPA exactly parallel to the component's position angle measured with respect to the core, was used to calibrate the EVPA. We estimate an error in the EVPA absolute orientation to be less than 5° for this epoch.

3. Results

Figures 2 and 3 show VLBA images of 3C 454.3 obtained with the VLBA at 22 and 43 GHz at the three epochs. Tables 1 and 2 summarize the physical parameters obtained for 3C 454.3. Tabulated data correspond to total flux density (S), polarized flux density (p), degree of polarization (m), EVPA (χ), separation (r) and structural position angle (θ) relative to the easternmost bright component [which we refer to as the "core" despite the fact that this component is not always bright (Marscher 1998) and may not be completely stationary (see below)], and angular size (FWHM). Components in the total intensity images were analyzed by model fitting the uv data with circular Gaussian components within the software Difmap (Shepherd, Pearson, & Taylor 1994). Components seen in the images of polarized intensity are not always coincident with maxima in total intensity (see also Kemball et al. 1996; Gómez et al. 1998), therefore we can only obtain estimates of m by the approximation that both maxima are coincident.

3.1. Source structure

Total intensity 1.3 cm images show a double component structure, very similar to that observed by Kemball et al. (1996) at 7 mm, consisting of the core and component *St*. This appears at a very similar separation from the core to that of component *2* in Pauliny-Toth et al. (1987), component *K7* of Cawthorne & Gabuzda (1996), and component *2* of Kemball et al. (1996). Hence, we identify it as the same stationary component, first detected in 1983.8 by Pauliny-Toth et al. (1987). We notice, however, that *St* seems to have been observed at different position angles from the core, from values close to $-100°$ measured by Pauliny-Toth et al. (1987) and Cawthorne & Gabuzda (1996), to about $-70°$ measured by Kemball et al. (1996), in closer agreement to the values we obtain. This is indicative of a swing toward the north in the inner jet between the 1980's and 1990's. Furthermore, our images show a systematic difference between the position angles and distances from the core of *St* for both observing wavelengths. This may be due to changes in the internal structure of *St* or the core — most probably the latter, since such changes are expected during the ejection of new components from the core. Indeed, our 7 mm images reveal the existence of component *A*, blended with the core in the corresponding 1.3 cm images.

Figure 3 also shows a component between the core and *St*, at a distance from the core in good accordance with that expected from extrapolating the motion of *A* between the previous two epochs (see Fig. 2). Therefore, we identify it as the same component, obtaining a proper motion relative to the core for the three combined epochs of μ=0.14 $\pm$0.02 mas yr^{-1}, which corresponds to an apparent speed of 2.9$\pm$0.4 $h^{-1}\,c$. Relative to component *St*, the proper motion is μ=0.18$\pm$0.02 mas yr^{-1}, or 3.9$\pm$0.4 $h^{-1}\,c$. In either case, the motion is significantly slower than that observed by Marscher (1998), who measured μ=0.28 $\pm$0.02 mas yr^{-1} for a component found at 43 GHz to be moving between the core and *St* during the period December 1994-October 1995. Unless the orientation with respect to the observer of the

inner jet in 3C 454.3 changed significantly between 1995 and 1996-1997, this would imply the ejection of components with intrinsically very different velocities in order to account for the differences in the observed proper motions. Even faster velocities were detected at larger scales by Pauliny-Toth (1998), whose observations at 5 and 8.4 GHz between 1984 and 1991.9 indicated a component moving along a curved path with a mean proper motion of μ=0.68 $\pm$0.02 mas yr^{-1}.

Assuming that A has maintained a constant speed since its ejection from the core, we estimate its birth at approximately 1995.7, coincident with a small outburst detected by the University of Michigan monitoring at 14.5 GHz[2] and Metsähovi Radio Research Station monitoring data at 22 and 37 GHz (Teräsranta et al. 1998). Kemball et al. (1996) observed a component — only detected in polarization — at a very similar separation from the core to that of A in July 1997, most probably associated with a previous ejection which they estimate took place at about 1994.4.

While component A does not show significant changes in flux during the three epochs, the core experienced a significant decrease in flux by about 1.5 Jy between the 1996.98 and 1997.58 epochs. Component *St* shows a very similar flux between both of the 1.3 cm epochs, however at 7 mm its flux progressively decreased, with a total variation of more than 2 Jy between the 1996.86 and 1997.58 epochs. Similar large variations of flux were also found in *St* by Pauliny-Toth et al. (1987) at 2.8 cm.

Beyond component *St*, Fig. 3 shows a complex jet structure, with emission extending to the north and south. Model fitting reveals a faint component in the north direction, which we have labeled n; it appears in the polarized intensity images as well. A lower resolution 15

[2]The University of Michigan Radio Astronomy Observatory is supported by the National Science Foundation and by funds from the University of Michigan.

GHz image presented by Kellermann et al. (1998) shows some indications of this structure in the form of a very extended core emission. 3C 454.3 is observed to extend initially to the west, presenting a relatively strong bend toward the northwest direction at about 4-5 mas from the core (Pauliny-Toth et al. 1987, Pauliny-Toth 1998; Cawthorne & Gabuzda 1996; Kellermann et al. 1998).

Figure 3 shows a faint extension of emission east of the core position. Unless it is due to calibration errors, its presence indicates emission upstream of the "core." A similar structure was first detected by Marscher (1998) in a series of 43 GHz VLBA images covering about two years, starting December 1994. Other indications of emission upstream of the core have also been found in high resolution 43 GHz VLBA images of 3C 120 (Gómez et al. 1998). A possible interpretation is that it corresponds to the actual region where the jet is being generated; such weak emission could be due to a lower flow Lorentz factor, as in the accelerating jet model of Marscher (1980), or associated with the birth of new moving components upstream of the core (Marscher 1998). In this case the core would represent a recollimation shock — strong in our observations and weak in 1995 when observed by Marscher (1998), as expected theoretically (Daly & Marscher 1988; Gómez et al. 1995).

3.2. Polarization

Polarized intensity images corresponding to the epochs at the end of 1996, shown in Fig. 2, reveal a sudden change in the polarized structure of the core at both observing frequencies in a 41-day interval. At 1.3 cm the core changes from being almost undetected in polarization, to showing a polarized flux of 78 mJy, with a degree of polarization of m=2.2%. This change in polarized flux is accompanied by a rotation of χ by almost 60°. At 7 mm we observe a very similar situation, in which the core and component A remain undetected in polarization at the 1996.86 epoch, but at 1996.98 appear with a degree of polarization for

the core similar to that observed at 1.3 cm, and a dramatic increase in polarization for A, with m=7.4%. Both the core and A show a similar χ to that observed at 1.3 cm for the core. The third 7 mm epoch reveals a rotation in χ of about 105° for component A, accompanied by a small decrease in m, while the core remained with a similar χ but a reduced percentage polarization to values similar to that corresponding to 1996.86 at 1.3 cm.

Component *St* is detected at all observing epochs and frequencies. Its degree of polarization maintains values between 1.3 and 2.2%, similar to that observed at 5 GHz by Cawthorne & Gabuzda (1996), except for the July 1997 epoch, in which it increases to 8.6%, close to that obtained by Kemball et al. (1996). Component *St* seems to have a frequency dependent EVPA. Our 7 mm images show χ close to the east-west direction, similar to that observed by Kemball et al. (1996). However, at 1.3 cm the EVPA of *St* presents a systematic offset of about 30–40° with respect to the values measured at 7 mm. Cawthorne & Gabuzda (1996) obtained a value of 29° in observations at 6 cm, which suggest a rotation of χ in *St* toward the north-south direction with increasing wavelength. Broten, Macleod, & Vallée (1988) obtained a rotation measure of -57 rad m^{-2} for 3C 454.3, which may account for the rotation of χ between our 1.3 cm values and those presented by Cawthorne & Gabuzda (1996). However, this small rotation measure would not affect our 1.3 cm and 7 mm observations, and consequently no Faraday rotation corrections have been made for the measured EVPA.

4. Theoretical interpretation and conclusions

4.1. Stationary component *St*

The existence of stationary and moving components in 3C 454.3 is also found in several other sources, e.g. in 4C 39.25 (Alberdi et al. 1993). In this case, the stationary component

is explained as being produced by a bend toward the observer, with the increased flux due to enhanced Doppler boosting. Similarly, we could explain the stationarity of *St* as due to a bend toward the line of sight. Indeed, the jet of 3C 454.3 is observed to bend toward the northwest direction at about 4-5 mas from the core (e.g., Pauliny-Toth et al. 1987, Pauliny-Toth 1998). In this case, a change in the apparent motion of component *A* is expected as it moves along the hypothetical bent trajectory, as observed and simulated in the case of 4C 39.25. Computing the proper motion of *A* between each pair of consecutive epochs, we find some evidence of deceleration as it moves closer to *St*, as well as a progressive, although small change in its position angle toward the northwest. With the information provided by the proper motion of *A* derived from the three epochs combined, we can estimate a maximum viewing angle of about 38°, and a minimum Lorentz factor of 3.07. In order to obtain a deceleration of *A* as produced by a bend toward the observer, the viewing angle must be significantly smaller than the maximum allowed, which final value depends on the actual Lorentz factor of *A*. In this case component *A* should also experience an increase in its flux, due to an enhancement of its Doppler boosting. However, only minor changes in the flux of *A* are observed across the three epochs. Of course, it is also possible that the apparent small deceleration of *A* could also result from a true change in its bulk Lorentz factor. However, the large error affecting the proper motion determination between the first two epochs prevents from drawing any solid conclusion regarding a possible deceleration of *A*.

The existence of a bend toward the observer in the region of *St* could also explain the large changes in flux experienced by this component, with no significant changes in its position and structure. A moving component should pass through *St*, giving during the interaction the impression of a single component with increasing flux, subsequently fading progressively as it passes *St* and turns around the bend (e.g., Gómez et al. 1994). Unless the the jet in *St* bends in a plane containing the observer, which is a priori unlikely, future

components that pass through *St* should move in a different direction in the plane of sky after the event.

Another possibility to explain the stationarity of *St* is that it is produced by a recollimation shock in the jet flow. Numerical simulations of the relativistic hydrodynamics and emission of jets have shown that pressure mismatches between the jet and the external medium may result in the generation of internal oblique shocks (Gómez et al. 1995, 1997). These shocks appear in the emission as stationary components due to the increased specific internal energy and rest-mass density. When a moving component passes through one of these recollimation shocks, both components would blend to appear as a single feature. This is accompanied by a "dragging" of the merged components downstream, because of the increase in the Mach number, as well as an enhancement of the emission. After the collision, the two components would split up, with the previously stationary component associated with the recollimation shock progressively fading and recovering its initial position and flux. The would give the appearance of motion upstream, as long as the initial physical conditions in the jet are recovered (Gómez et al. 1997). Within this scenario, a moving component would not experience significant changes in its proper motion and flux as it approached the stationary component, similar to what is observed for *A*. This would give the impression of a quiescent merge of the two components. A similar situation, accompanied by a brief dragging of the stationary component, was observed for the merging of components *K1* and *K2* by Gabuzda et al. (1994) in the BL Lac object 0735+178. In the case of a strong standing shock, as perhaps produced by a sudden change in the external medium pressure, more violent interactions with moving shocks may be expected.

We propose a consistent scenario for the inner region in 3C 454.3 in which both the core and component *St* represent strong recollimation shocks. When new components are generated, they should increase significantly the emission of the core, briefly dragging its po-

sition downstream. This interpretation is in very good agreement with the observations by Marscher (1998). These show a roughly stationary component, labeled S2 (corresponding to the component marked as the core in this paper) at about 0.2 mas downstream of the eastern end of the jet. New superluminal components seem to appear upstream of S2, which could explain the emission upstream of the core in Fig. 3. These observations also showed a slight motion downstream of S2, before it recovered its initial position as a moving component passes it, as predicted by the theory (Gómez et al. 1997). A similar interaction would be expected when the moving component reaches the position of the next recollimation shock, corresponding to *St*. The large changes in the flux of *St* could then be explained by these interactions. However, in order to test this model, accurate measurements of the absolute positions of components are needed, possible through a careful high resolution phase-reference monitoring program. They should provide the necessary information to confirm the constancy of the core–*St* separation (within the expected motions due to the passage of moving components) and the emergence and evolution of new components upstream of the core.

Cawthorne & Cobb (1990) showed that, depending on the jet flow Lorentz factor and the orientation with respect to the observer, conical shocks may show a polarization position angle parallel or perpendicular to the jet flow. In the limit of strong shocks, this would require small viewing angles, as measured in the rest frame of the shock, to explain the aligned EVPA with respect to the projected direction of the jet observed for the core and *St*.

Tables 1 and 2 reveal an optically thin spectrum for component *St* at both 1996 epochs, which eliminates opacity effects as being responsible for the systematic offset observed in the EVPA at different wavelengths. The observed EVPA for component *St* at 1.3 cm differs only by about 20° from that measured by Cawthorne & Gabuzda (1996) at 6 cm. Some of this discrepancy may be explained by Faraday rotation, which at 6 cm would produce a rotation of

$\sim -12^{\circ}$ (Broten, Macleod, & Vallée 1988). Hence, the measured difference in the EVPA these authors observed between *St* and the outer components is probably due to an intrinsically different nature, rather than to opacity effects. A possibility is that the outer components Cawthorne & Gabuzda (1996) observed represent weak plane-perpendicular moving shocks in a predominantly longitudinal magnetic field configuration. These shocks will slightly enhance the perpendicular component of the magnetic field (parallel to the shock front), but the increase will not be enough to overcome the initial longitudinal field. Hence the final net orientation of the field would remain aligned in the direction of the jet flow. As a consequence of the partial cancellation of the magnetic field produced by the shocks, a small degree of polarization is expected, which contrasts with the large values measured by Cawthorne & Gabuzda (1996) for the outer components. This cannot be applied to *St*, and we need to consider a different interpretation in terms of a conical shock or a bend, as outlined previously. If *St* corresponds to a bend, no changes in the EVPA are expected as a consequence of the change in curvature along the bent portion of the jet, and we need to assume an underlying perpendicular magnetic field for *St* to explain the observed EVPA, as opposed to that measured downstream by Cawthorne & Gabuzda (1996). Another possibility, still under the hypothesis of a bend along the position of *St*, is that there is another moving plane perpendicular shock component passing through it, such that *St* represents the blended component, whose parallel EVPA is due to the enhancement by the shock of the perpendicular component of the magnetic field. However, it seems unlikely to have such a situation each time the source has been observed. In the case that *St* corresponds to an oblique shock, the observed EVPA can still be explained without needing to assume a change in the underlying magnetic field of *St* with respect to the outer components, in which case the magnetic field would be aligned with the jet axis throughout the entire jet. Depending on the jet flow Lorentz factor and viewing angle, Cawthorne & Cobb (1990) showed that a conical shock may exhibit an EVPA aligned with the jet axis. Those results were obtained

considering an initially randomly oriented magnetic field, and need to be confirmed in the case of an initially aligned field.

4.2. Polarized outburst in superluminal component A

The polarized structural outburst observed in the 1996 epochs may be explained by assuming that, at the 1996.86 epoch, the EVPA of the core and component A were mutually perpendicular, producing a net cancellation of the polarized intensity. In this case, component A is required to have changed its EVPA by almost a full rotation of 90°, making it approximately aligned with that of the core – assumed to remain with an approximately constant EVPA — which led to the sudden appearance of both components in the polarized intensity images at 1996.98. Taking into account that the apparent core at 1.3 cm in fact corresponded to blending of the core and component A, the resulting spectrum is rather flat, and we could assume that the rotation of 90° in the EVPA of A may be due to a change from being optically thick at 1996.86, to optically thin at 1996.98. We shall also note that the lack of polarization in the core region at the first epoch may be due to large opacity values. However, the fact that A remained undetected at 22 GHz prevents us from obtaining a reliable determination of its spectrum, and hence its opacity. It is also possible that the burst in polarization may result from drastic changes in the magnetic field configuration.

This represents a remarkably rapid change in the polarized structure of component A. From the timescale of variability, we can derive an upper limit to the size of A as $R_{\rm max} = c\, t_{\rm var}\, [\delta/(1+z)]$, where δ is the Doppler factor. Using the minimum Lorentz factor of 3.07 derived from the proper motion, and assuming a viewing angle of $1/\Gamma$, which maximizes the apparent velocity, we obtain a maximum size of $\sim$10 μas. Model fitting component sizes tabulated in table 2 show that only for epoch 1997.58 can the size of component A be measured, with an estimated FWHM of 190 μas, well above the derived maximum. We shall

note however, that we cannot rule out that the observed variability may arise from the core. In this case the estimated sizes tabulated in Table 2 are very similar and also above the estimated maximum, except for epoch 1996.86 in which model fitting yields a delta-function component for the core. We therefore conclude that the Doppler factor must be higher than the minimum implied by these observations, and instead must be similar to those suggested by the faster proper motions observed by Marscher (1998) and Pauliny-Toth (1998).

If component A changed its opacity from optically thick to thin between 1996.86 and 1996.98, it seems less plausible to assume that A became thick again in 1997.58, as would be required if we were to explain the further rotation of 90° in its EVPA in this way. To account for this extra rotation, we need to assume a change in the magnetic field of the underlying jet or in component A. If component A is associated with a moving plane-perpendicular shock, we expect an EVPA aligned with the direction of the jet flow when the component is optically thin. This could explain the value of χ observed in 1996.98. Since the underlying magnetic field remains aligned with the jet axis through the jet of 3C 454.3, as seems to be deduced from the outer components observed by Cawthorne & Gabuzda (1996), the rotation of 90° in the EVPA of A could be explained by assuming that the strength of the shock associated with it decreases as the component moves downstream. In 1996.98 the enhancement of the perpendicular component of the magnetic field produced by the shock associated with A would overcome the initial longitudinal field direction. However, once the shock has moved to the position observed in 1997.58, we find that the enhancement of the perpendicular field by a weaker shock would not be enough to change the initially aligned net field of the underlying jet, resulting in a net magnetic field parallel, and an EVPA perpendicular, to the jet axis. However, it then remains unclear why component A maintained a similar flux — even experiencing a small increase, as opposed to what it would be expected in the case of a decrease in the shock strength. Within this scenario, component St would be required to be associated with a conical shock in order to obtain a net magnetic field perpendicular to

the jet axis (assuming no magnetic field changes between the positions of *A* and *St*).

Further polarimetric high-resolution VLBA observations are required to test these hypotheses. The study would be improved significantly by performing phase-reference to an external source, allowing a detailed determination of the proper motions of components. These would be of great importance to test our hypothesis of recollimation shocks to interpret the nature of *St* and possibly the core. In this case, numerical simulations predict a temporary drag of these components, followed by a brief upstream motion to recover their initial positions (Gómez et al. 1997). Polarimetric observations would provide the necessary information to discern between a possible rotation of the underlying magnetic field configuration, or a change in the strength of shocks in the inner structure of 3C 454.3.

This research was supported in part by Spain's Dirección General de Investigación Científica y Técnica (DGICYT), grants PB94-1275 and PB97-1164, by NATO travel grant SA.5-2-03 (CRG/961228), by U.S. National Science Foundation grant AST-9802941, and by NASA through CGRO Guest Investigator Program grants NAG5-2508, NAG5-3829, and NAG5-7323 and RXTE Guest Investigator Program grants NAG5-3291, NAG5-4245, and NAG5-7338.

REFERENCES

Alberdi, A., Marcaide, J. M., Marscher, A. P., Zhang, Y. F., Elósegui, P., Gómez, J. L., & Shaffer, D. B. 1993, ApJ, 402, 160

Broten, N. W., Macleod, J. M., & Vallée, J. P. 1988, Ap&SS, 141, 303

Cawthorne, T. V., & Cobb, W. K. 1990, ApJ, 350, 536

Cawthorne, T. V., & Gabuzda, D. C. 1996, M.N.R.A.S., 278, 861

Cotton, W. D., Geldzahler, B. J., Marcaide, J. M., Shapiro, I. I., Sanromá, M., & Rius, A. 1984, ApJ, 286, 503

Daly, R. A., & Marscher, A. P. 1988, ApJ, 334, 539

Gabuzda, D. C., Wardle, J. F. C., Roberts, D. H., Aller, M. F., & Aller, H. D. 1994, ApJ, 435, 128

Gómez, J. L., Alberdi, A., Marcaide, J. M., Marscher, A. P., & Travis, J. P. 1994, A&A, 292, 33

Gómez, J. L., Martí, J. M., Marscher, A. P., Ibáñez, J. M., & Marcaide, J. M. 1995, ApJ, 449, L19

Gómez, J. L., Martí, J. M., Marscher, A. P., Ibáñez, J. M., & Alberdi, A. 1997, ApJ, 482, L33

Gómez, J. L., Marscher, A. P., Alberdi, A., Martí, J. M., & Ibáñez, J. M. 1998, ApJ, 499, 221

Kellermann, K. I., Vermeulen, R. C., Zensus, J. A., & Cohen, M. H. 1998, ApJ, 115, 1295

Kemball, A. J., Diamond, P. J., & Pauliny-Toth, I. I. K. 1996, ApJ, 464, L55

Leppänen, K. J., Zensus, J. A., & Diamond, P. J. 1995, AJ, 110, 2479

Marscher, A. P. 1980, ApJ, 235, 386

Marscher, A. P. 1998, in IAU Colloq. 164, Radio Emission from Galactic and Extragalactic Compact Sources, ed. J. A. Zensus, J. M. Wrobel, & G. B. Taylor (San Francisco: ASP), p. 25

Pauliny-Toth, I. I. K., Porcas, R. W., Zensus, J. A., Kellermann, K. I., Wu, S. Y., Nicolson, G. D., & Mantovani, F. 1987, Nature, 328, 778

Pauliny-Toth, I. I. K. 1998, in IAU Colloq. 164, Radio Emission from Galactic and Extragalactic Compact Sources, ed. J. A. Zensus, J. M. Wrobel, & G. B. Taylor (San Francisco: ASP), p. 75

Shepherd, M. C., Pearson, T. J., & Taylor, G. B. 1994, BAAS, 26, 987

Teräsranta, H. et al. 1998, A&AS, 132, 305

This manuscript was prepared with the AAS LaTeX macros v4.0.

Fig. 1.— VLBA images of 0420-014 at 22 GHz at epochs 1996 November 11 (*top left*) and 1996 December 22 (*top right*), and 43 GHz at 1996 November 11 (*bottom left*) and 1996 December 22 (*bottom right*). Total intensity is plotted as contour maps, while the linear gray scale shows the linearly polarized intensity. The superposed sticks give the direction of the electric field vector. From *top left* to *bottom right* images: contour levels are in factors of 2, starting at [of peak intensity] 0.5 [3.15], 0.2 [6.5], 0.25 [3.45] and 0.2% [1.7 Jy beam^{-1}]; convolving beam [position angle]: 0.67×0.32 [-1°], 0.69×0.31 [-1°], 0.39×0.17 [-2°] and 0.39×0.17 (FWHM) [-2°] mas; maximum in polarized intensity [noise level]: 51 [5], 78 [23], 49 [10] and 37 [7] mJy beam^{-1}.

Fig. 2.— Same as Fig. 1 but for 3C 454.3. From *top left* to *bottom right* images: contour levels are in factors of 2, starting at [of peak intensity] 3 [2.49], 2 [3.03], 2 [2.1] and 2% [2.45 Jy beam^{-1}]; convolving beam [position angle]: 0.75×0.27 [-1°], 0.79×0.31 [-2°], 0.39×0.14 [-2°] and 0.39×0.15 (FWHM) [-2°] mas; maximum in polarized intensity [noise level]: 58 [20], 84 [9], 33 [6] and 83 [8] mJy beam^{-1}.

Fig. 3.— Same as Fig. 1 for 3C 454.3, epoch 1997 July 30 at 43 GHz. Contour levels are in factors of 2, starting at 0.5% (including -0.5%) of the peak of 0.94 mJy beam^{-1}. The convolving beam is 0.342×0.151 mas (FWHM), with position angle -1°, and the maximum in polarized intensity is 69 mJy beam^{-1}, with a noise level of 6.9 mJy beam^{-1}.

Table 1. 22 GHz models for 3C 454.3.

Component	S (Jy)	p (mJy)	m (%)	χ (°)	r (mas)	θ (°)	FWHM (mas)
			1996.86				
Core	3.11	26	0.8	178	...	...	0.23
St	4.54	59	1.3	50	0.51	-67	0.37
			1996.98				
Core	3.59	78	2.2	120	...	...	0.21
St	4.61	86	1.8	47	0.53	-66	0.38

Table 2. 43 GHz models for 3C 454.3.

Component	S (Jy)	p (mJy)	m (%)	χ (°)	r (mas)	θ (°)	FWHM (mas)
			1996.86				
Core	2.09	...	...	...	...	...	0
A	1.48	...	...	...	0.16	-93	0
St	3.59	78	2.2	81	0.62	-72	0.39
			1996.98				
Core	2.53	55	2.2	96	...	...	0.03
A	1.16	86	7.4	125	0.18	-87	0
St	2.45	34	1.4	89	0.61	-71	0.38
			1997.58				
Core	0.92	9	0.9	109	...	...	0.03
A	1.28	68	5.2	20	0.26	-85	0.19
St	1.50	100	8.6	93	0.59	-70	0.42
n	0.13	1.5	4.3	10	1.13	-39	0.18

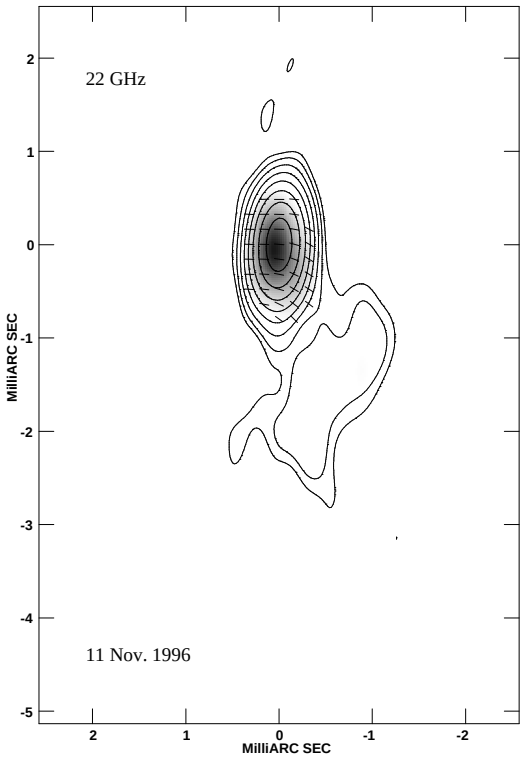
22 GHz
11 Nov. 1996
MilliARC SEC
MilliARC SEC

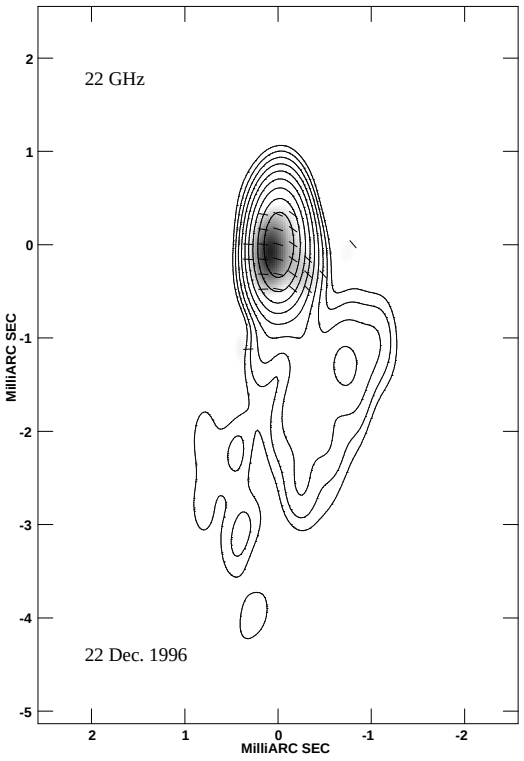
22 GHz
22 Dec. 1996
MilliARC SEC
MilliARC SEC

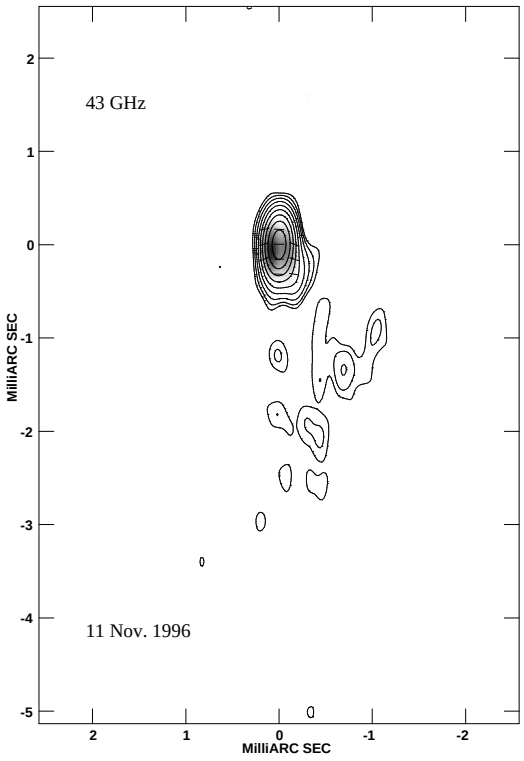
43 GHz
11 Nov. 1996
MilliARC SEC
MilliARC SEC

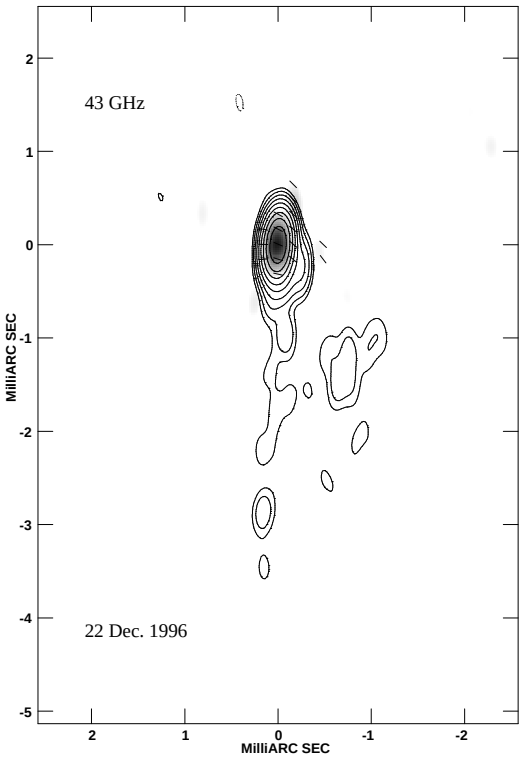
43 GHz
22 Dec. 1996
MilliARC SEC
MilliARC SEC

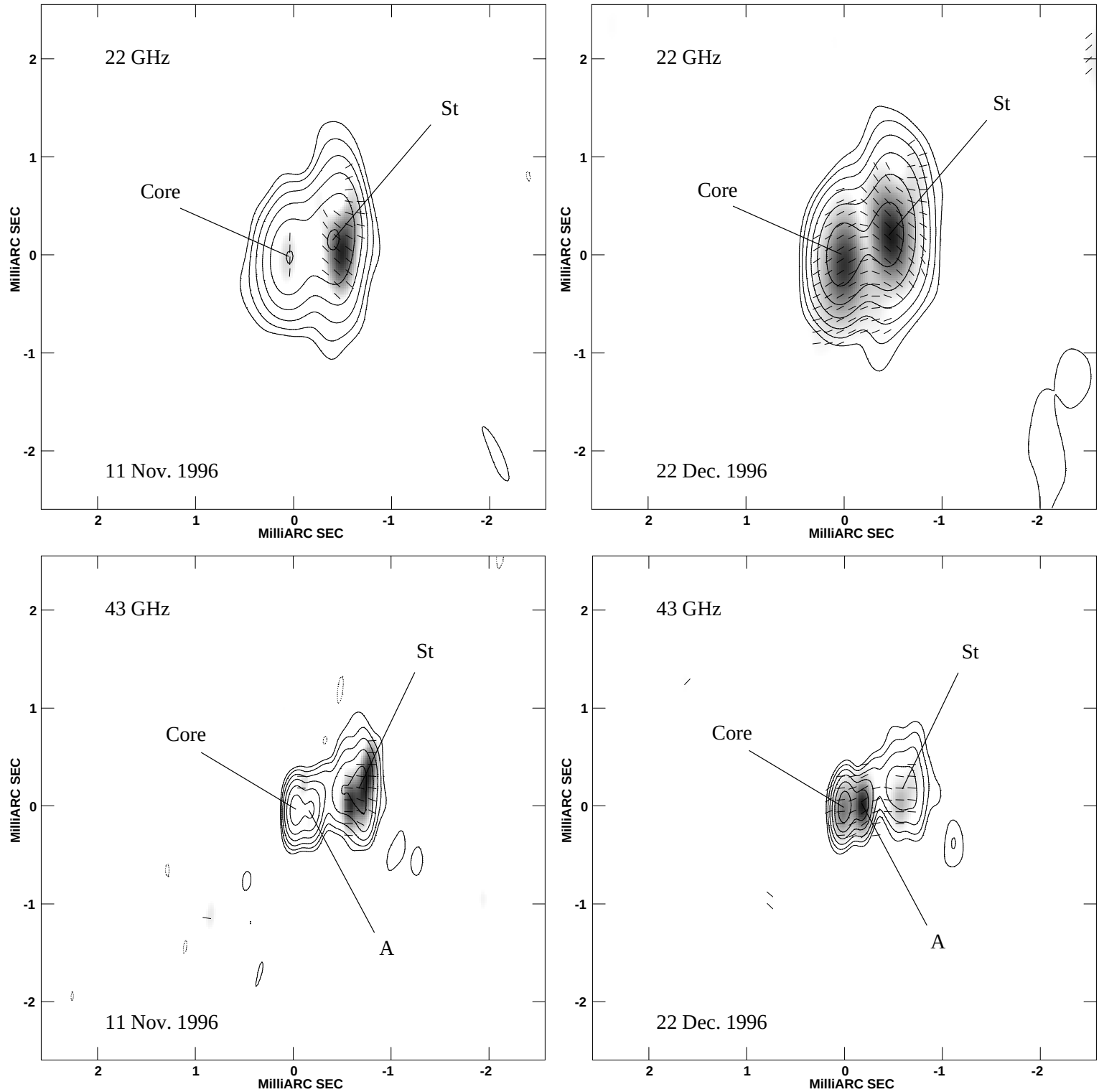
22 GHz
St
Core
11 Nov. 1996
MilliARC SEC
22 GHz
St
Core
22 Dec. 1996
MilliARC SEC
43 GHz
St
Core
A
11 Nov. 1996
MilliARC SEC
43 GHz
St
Core
A
22 Dec. 1996
MilliARC SEC

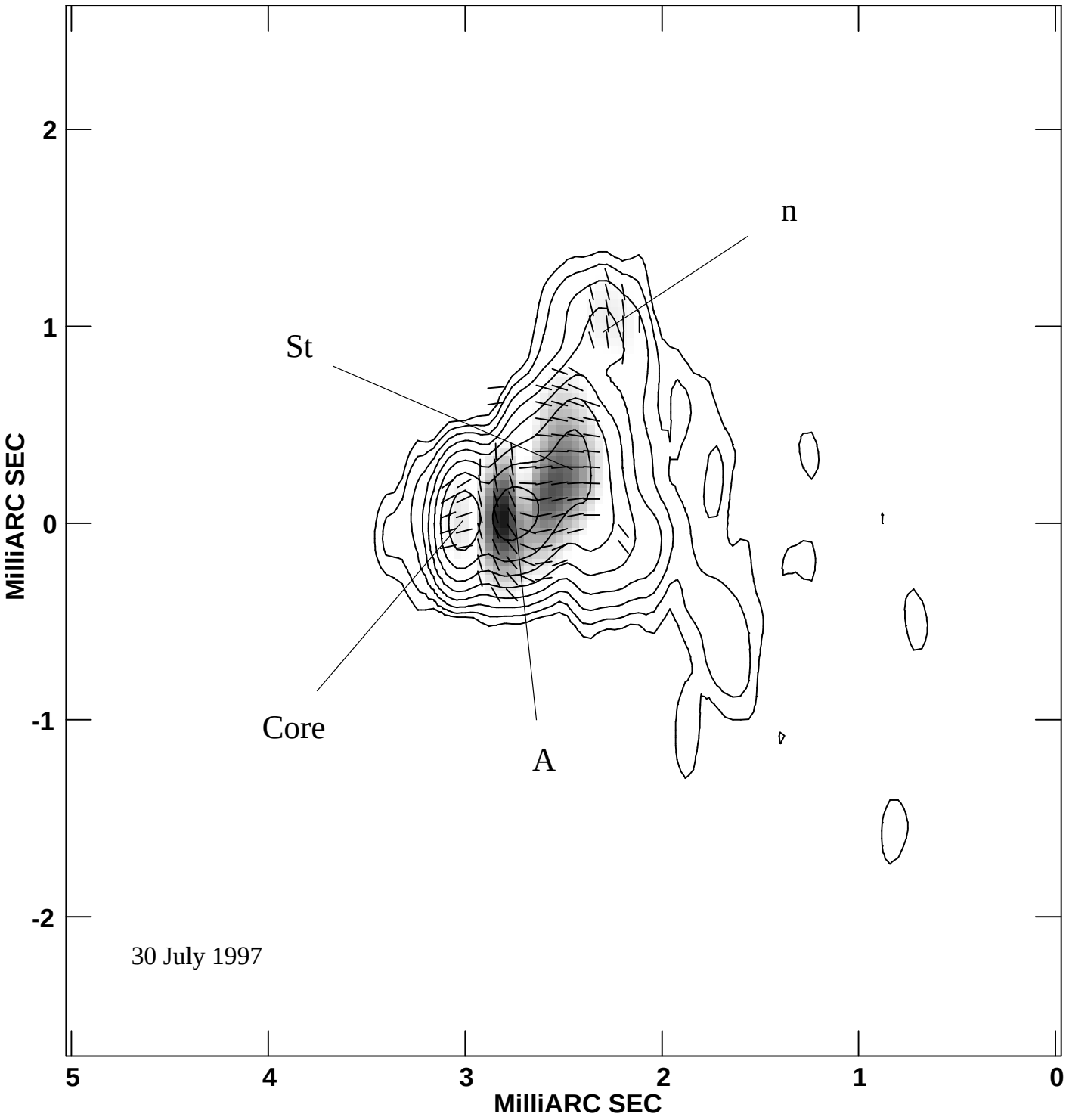
n
St
Core
A
30 July 1997
2
1
0
-1
-2
MilliARC SEC
5
4
3
2
1
0
MilliARC SEC